Supplement

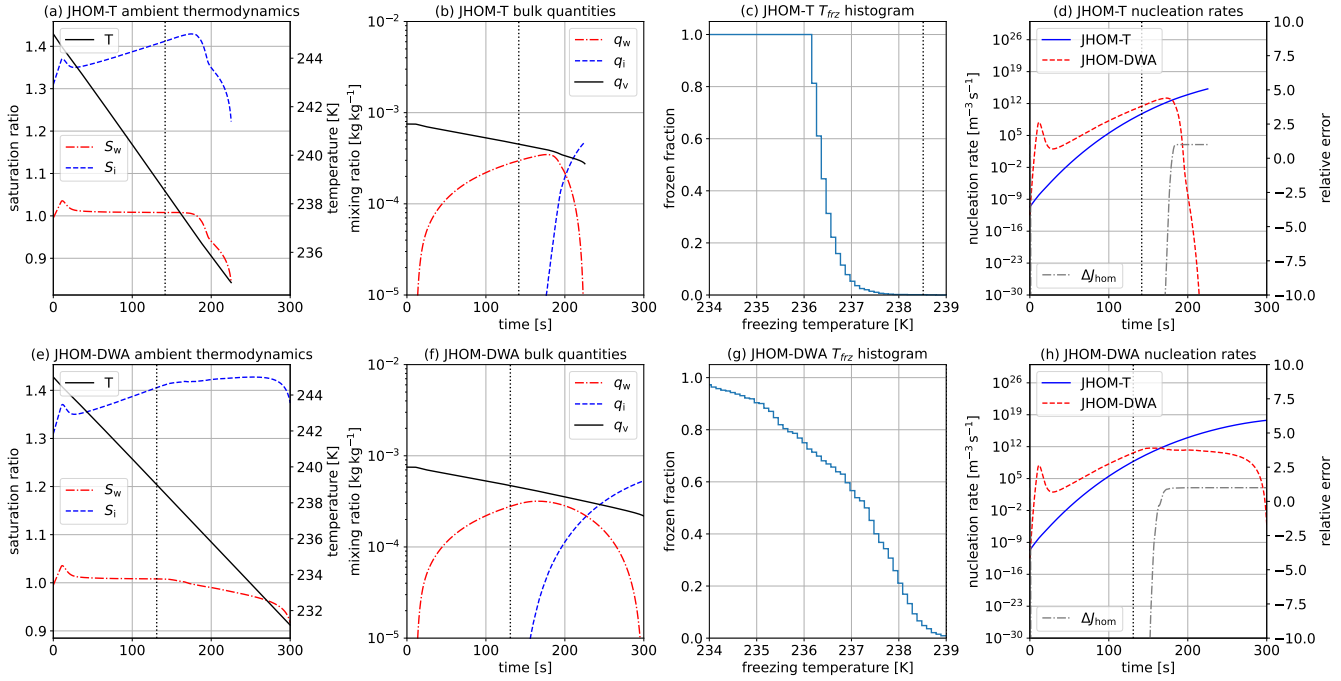

Figure S1. Air parcel ascent simulations with vapour deposition on ice active using JHOM-T (a–d) and JHOM-DWA (e–h) homogeneous nucleation rate formulations, showing (a, e) ambient temperature T and saturation ratios S_w and S_i, (b, f) bulk quantities, (c, g) freezing temperature histograms, and (d, h) nucleation rates. The dashed line indicates the first freezing event.

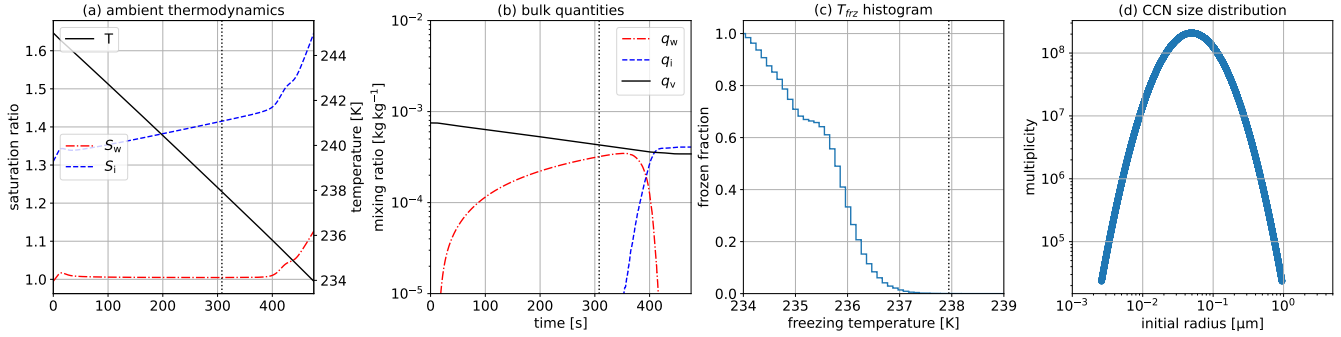

Figure S2. Air parcel ascent simulations for a lognormal CCN spectrum showing (a) ambient temperature T and saturation ratios S_w and S_i, (b) bulk quantities, (c) freezing temperature histogram, and (d) initial CCN size distribution. The dashed line indicates the first freezing event.

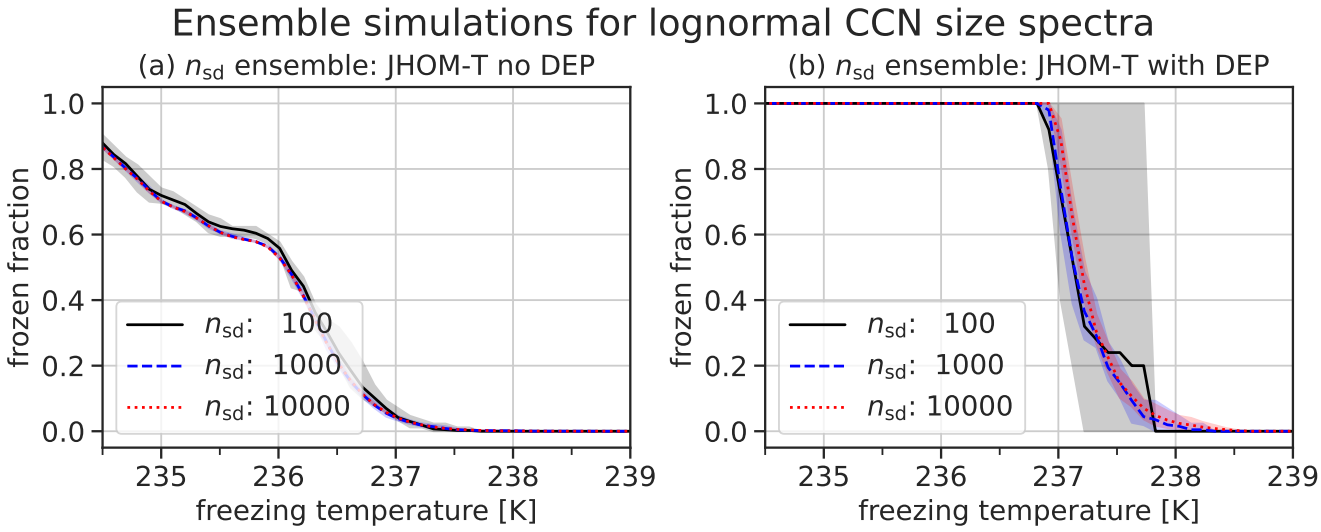

Figure S3. n_{sd} ensemble simulations using the JHOM-T nucleation rate without (a) and with (b) vapour deposition on ice. A lognormal CCN size distribution with $\sigma = 2$ is used instead of a monodisperse spectrum.

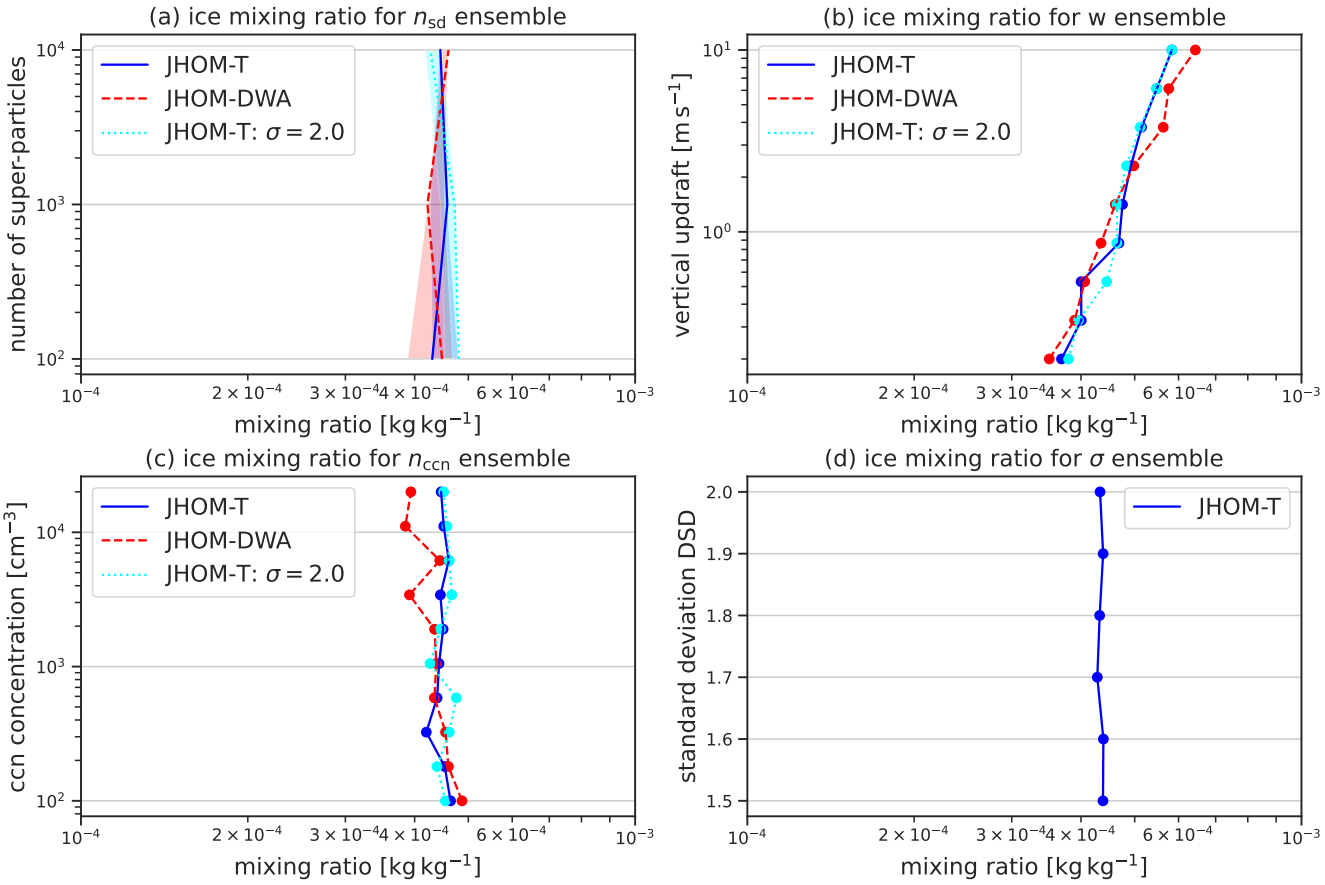

Figure S4. Bulk ice mixing ratio q_i for (a) the n_{sd} ensemble, (b) the w ensemble, (c) the n_{ccn} ensemble, and (d) the σ ensemble. Blue lines indicate simulations using the JHOM-T nucleation rate with monodisperse CCN spectra, teal lines the JHOM-T rate with lognormal CCN spectra, and red lines simulations using the JHOM-DWA rate.

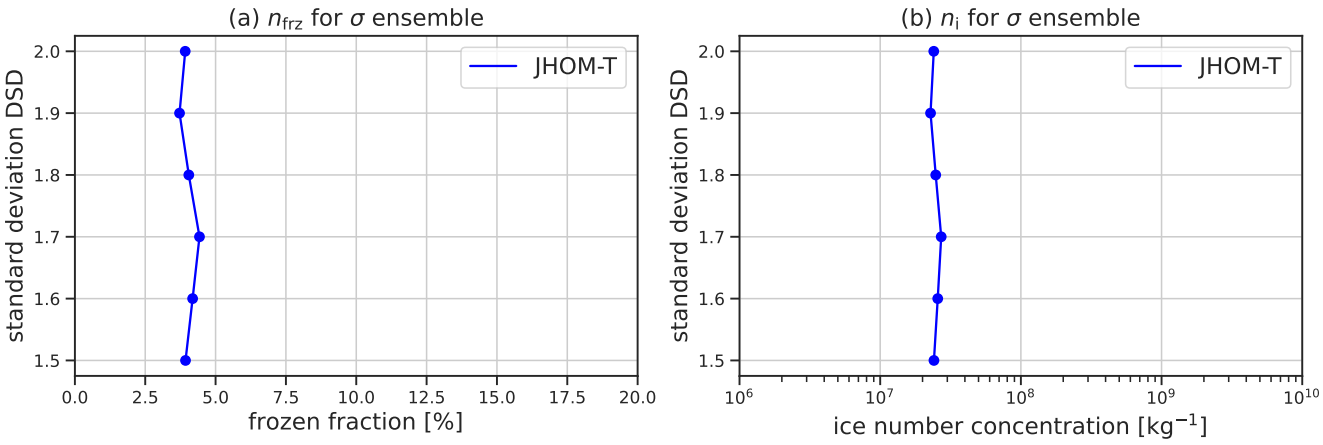

Figure S5. (a) frozen fraction n_{frz} and (b) ice number concentration n_i for the σ ensemble using the JHOM-T nucleation rate.